SCIENCE CHINA
Physics, Mechanics & Astronomy

• Research Paper •

May 2010 Vol.53 No.5: 802–806
doi: 10.1007/s11433-010-0175-1

Effects of viscosity on shock-induced damping of an initial sinusoidal disturbance

MA XiaoJuan[1], LIU FuSheng[1*] & JING FuQian[2]

[1] *College of Physical Science and Technology, Southwest Jiaotong University, Chengdu 610031, China;*
[2] *Laboratory for Shock Wave and Detonation Physics Research, Institute of Fluid Physics, Chinese Academy of Engineering Physics, Mianyang 621900, China*

Received December 23, 2009; accepted March 9, 2010

A lack of reliable data treatment method has been for several decades the bottleneck of viscosity measurement by disturbance amplitude damping method of shock waves. In this work the finite difference method is firstly applied to obtain the numerical solutions for disturbance amplitude damping behavior of sinusoidal shock front in inviscid and viscous flow. When water shocked to 15 GPa is taken as an example, the main results are as follows: (1) For inviscid and lower viscous flows the numerical method gives results in good agreement with the analytic solutions under the condition of small disturbance (a_0/λ=0.02); (2) For the flow of viscosity beyond 200 Pa s ($\eta = \kappa$) the analytic solution is found to overestimate obviously the effects of viscosity. It is attributed to the unreal pre-conditions of analytic solution by Miller and Ahrens; (3) The present numerical method provides an effective tool with more confidence to overcome the bottleneck of data treatment when the effects of higher viscosity in experiments of Sakharov and flyer impact are expected to be analyzed, because it can in principle simulate the development of shock waves in flows with larger disturbance amplitude, higher viscosity, and complicated initial flow.

viscosity coefficient, two-dimensional Eulerian flow, shock front, sinusoidal disturbance

PACS: 66.20.Cy, 47.40.-x, 62.50.+p

Viscosity of substance at high pressures is important for the description of dynamic evolution in the deeper earth [1,2] and of flow development of shock waves [3,4], which is described by shear and bulk coefficients in Newtonian viscous fluid theory [5]. However, data of these quantities are very lacking for metals and silicates because direct measurements become very difficult at high pressures of Mbar and high temperatures of several thousand Kelvin.

The so-called oscillatory damping method was put forward for such an extreme condition, which relies on the correlation between viscosity of shock compressed state and amplitude damping and oscillation of an initial sinusoidal disturbance on shock front in concerned substance. Sakharov and Mineev et al. [4,6–9] especially designed experiments for generating shock waves with sinusoidal geometrical disturbance on front and measuring the amplitude damping and oscillation by a combination of explosive loading and high-speed imaging techniques. In their analysis, Zaidel's [10] analytic solution for the disturbance development of shock front were adopted to constrain the shear viscosity coefficients of several materials. Two decades later, Miller and Ahrens [5] re-examined Zaidel's approximations in details. They considered the effect of bulk viscosity, and got an analytic solution for a more general non-uniform initial condition. It should be pointed out that some preconditions were still put on their solution: (a) weak viscosity; (b) small-amplitude disturbance; (c) ideal discontinuity of the shock front; (d) a simple initial flow. These harsh requirements can not be satisfied in actual experiments [4,6–9,11–13], so a lack of a widely used and reliable data analysis method has been the bottleneck of viscosity

*Corresponding author (email: fusheng_1@163.com)

measurement for a long time.

In this article, the finite difference method is applied to solve the hydrodynamic equations of two-dimensional Eulerian flow, and the propagation of shock waves with initial sinusoidal front is followed by a shock capturing scheme of maximum pressure gradients. From the geometrical shape of shock front and its development with shock propagation the numerical solution of the sinusoidal disturbance amplitude damping curve is firstly obtained, and the viscosity effects behind the shock front on it will be discussed.

1 Finite differenced method

The two-dimensional Eulerian form of hydrodynamic equations [5] (including mass, momentum, and energy equation) can be expressed as

$$\frac{\partial \rho}{\partial t}+u_x\frac{\partial \rho}{\partial x}+u_z\frac{\partial \rho}{\partial z}=-\rho\left(\frac{\partial u_x}{\partial x}+\frac{\partial u_z}{\partial z}\right), \tag{1}$$

$$\begin{cases}\rho\left(\dfrac{\partial u_x}{\partial t}+u_x\dfrac{\partial u_x}{\partial x}+u_z\dfrac{\partial u_x}{\partial z}\right)=\dfrac{\partial \tau_{xx}}{\partial x}+\dfrac{\partial \tau_{xz}}{\partial z},\\ \rho\left(\dfrac{\partial u_z}{\partial t}+u_x\dfrac{\partial u_z}{\partial x}+u_z\dfrac{\partial u_z}{\partial z}\right)=\dfrac{\partial \tau_{zz}}{\partial z}+\dfrac{\partial \tau_{xz}}{\partial x},\end{cases} \tag{2}$$

$$\begin{aligned}&\rho\left(\frac{\partial E}{\partial t}+u_z\frac{\partial E}{\partial x}+u_z\frac{\partial E}{\partial z}\right)\\ &\quad=\tau_{xx}\frac{\partial u_x}{\partial x}+\tau_{zz}\frac{\partial u_z}{\partial z}+\tau_{xz}\left(\frac{\partial u_x}{\partial z}+\frac{\partial u_z}{\partial x}\right),\end{aligned} \tag{3}$$

where ρ and E are density and energy of the shocked material, respectively, u_x, u_z are the particle velocity in the x and z directions. The stress tensor [14] in the (x, z) coordinate frame is given by the components:

$$\begin{cases}\tau_{xx}=-P+q+\dfrac{2}{3}\eta\left(2\dfrac{\partial u_x}{\partial x}-\dfrac{\partial u_z}{\partial z}\right)+\kappa\left(\dfrac{\partial u_x}{\partial x}+\dfrac{\partial u_z}{\partial z}\right),\\ \tau_{xz}=\tau_{zx}=\eta\left(\dfrac{\partial u_z}{\partial x}+\dfrac{\partial u_x}{\partial z}\right),\\ \tau_{zz}=-P+q+\dfrac{2}{3}\eta\left(2\dfrac{\partial u_z}{\partial z}-\dfrac{\partial u_x}{\partial x}\right)+\kappa\left(\dfrac{\partial u_x}{\partial x}+\dfrac{\partial u_z}{\partial z}\right),\end{cases} \tag{4}$$

where P is the pressure, η is the shear viscosity, κ is the bulk viscosity, and q is expressed as [14]

$$q=m\rho\frac{\partial u_x}{\partial x}\quad\text{or}\quad q=m\rho\frac{\partial u_z}{\partial z}, \tag{5}$$

where m is artificial viscosity coefficient which is used to suppress the numerical noise and meet the requirement of flow continuity at the shock front [15].

The above constitutive equations are differenced by Mader [14] and numerically solved by a program coding written according to the given steps.

The reference frame and the gridding scheme are shown in Figure 1, the length of direction x and z is 30 and 10 mm, respectively, and the shock wave is assumed to go along the x-axis. The sinusoidal geometrical disturbance with wavelength λ and initial amplitude a_0 is added to the planar shock front. The non-uniform initial flow suggested by Miller and Ahrens [5] is adopted, in which the disturbances of the velocity and the pressure are added to the flow field behind the shock front.

$$\begin{cases}u_x=-k_0va_0S\dfrac{(\sigma-1)(1+\delta)}{\sigma(1-\delta)}\mathrm{e}^{-\alpha\Delta x}\cos(k_0z),\\ u_z=k_0va_0(\sigma-1)\mathrm{e}^{-\alpha\Delta x}\sin(k_0z),\\ P=-k_0va_0S\dfrac{2(\sigma-1)}{\sigma(1-\delta)}\mathrm{e}^{-\alpha\Delta x}\cos(k_0z),\end{cases} \tag{6}$$

where k_0 (=2π/λ) is the wave vector, σ is the ratio of compression, a_0 is the initial shock disturbance amplitude, Δx is the distance away from the front, S depicts the intensity of disturbance, α describes the attenuation rate of the perturbed amplitude, and $\delta=[\sigma-s(\sigma-1)]/[\sigma+s(\sigma+1)]$, s is parameter in the linear relationship between mass and shock velocity: $D=c_0+su$.

The un-shocked part of flow has normal pressure P_0, initial densityρ_0, and its particle velocity value being zero. The corresponding values of these quantities of the shocked part are derived from the Rankine-Hugoniot relations.

The continuum boundary is applied to the left and right sides, and the periodic condition is assumed for up and down boundaries to assure the periodicity of disturbance, i.e. the simulation length in the z direction is right the wavelength λ of the disturbance.

2 Shock capturing scheme

To study the evolution of disturbed shock waves, it is important to continuously capture the positions of the shock

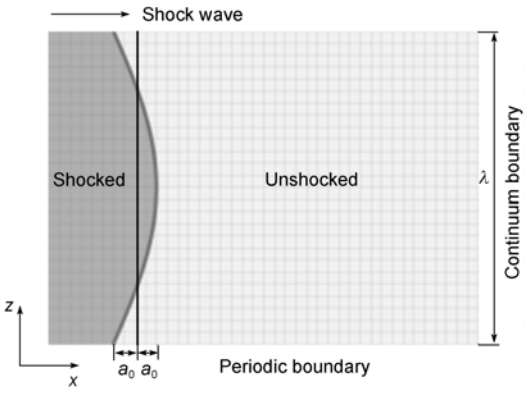

Figure 1 The gridding scheme and boundary condition.

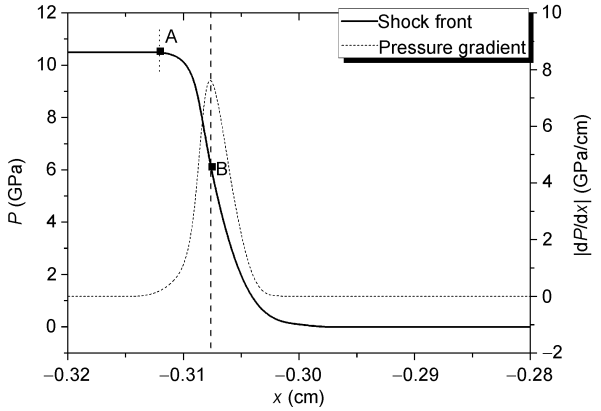

Figure 2 The capturing method of shock wave and the pressure gradient absolute value.

front, which has a finite width because of artificial viscosity. In the present work, a capturing scheme of maximum pressure gradient along the x-axis is used to locate the position of the shock front as shown in Figure 2. The pressure gradient along each horizontal gridding line is determined by a polynomial smooth fit $P(x)$, then the B on the shock front, which has the same x value as the peak point on the pressure gradient absolute value curve, is an indicator for the position of the shock front.

The disturbance development on the shock front is figured out in the x-z plane by lining up the indicative points B of the shock front. The displacement of shock waves and the amplitude of disturbance on front are determined by fitting these points to a sinusoidal oscillatory function with the same wavelength of initial disturbance: $f=x+a\cos(2\pi z/\lambda)$.

3 Consideration of viscosity

In analytic solution of Miller and Ahrens [5] the shock front is supposed to be a "discontinuity interface" without any width which is inconsistent with actual experiments, and only the flow behind the shock front is treated as Newtonian viscous fluid. However, in numerical simulation of the present work the shock front is of finite width depending on the size of gridding element and the value of artificial viscosity coefficient. According to the pressure gradient absolute value, the shock-compressed flow is separated into the region of shock front and the region behind the shock, between them a boundary is labeled by point A, where the pressure gradient values zero and it is close to the front, as can be seen in Figure 2.

To investigate the effects of viscosity on the development of sinusoidally disturbed shock waves, two different kinds of viscosity coefficients are coupled into hydrodynamic equations of viscous flow. When the artificial viscosity originated with von Neumann [15] values 1×10^4 Pa s, the shock front spread in several grids and the numerical noise is suppressed very well. In region behind the shock the strain rates keep on the controlled level by disturbance, so the real viscosity can be approximately described by Newtonian theory of viscous flow, but not in the shock front region because of changing several orders of magnitude in strain rate, and the details would be known if the pressure history was precisely measured by VISAR technique with high time resolution [16] according to the dislocation dynamic theory.

So as a simplification, the artificial viscosity takes effect to control the pressure rise within the shock front, the real viscosity in the shock front region is set to zero, and only exists behind of front. Thus the focus in this paper is to investigate the effects of viscosity behind the shock front on the evolution of sinusoidal disturbance amplitude. This treatment also makes our numerical results comparable to the analytic solution of Miller and Ahrens. During simulation, the location of point A is optimized to evaluate the ultimate effects of viscosity in region behind the shock on disturbance amplitude of the shock front, while the monotonic shock wave must keep steady.

4 Numerical solutions

In this article, water [7], shocked to 15 GPa, is taken as an example, as Miller and Ahrens did. Equation of state (EOS) of water is given by its Hugoniot EOS and Gruneisen EOS. Its initial density is ρ_0, and Hugoniot parameters c_0 and s respectively values are 0.998 g/cm^3, 2.393 km/s and 1.333 [17]. Its Gruneisen parameter γ_0 at initial state values 0.5, and $\rho\gamma=\rho_0\gamma_0$ is supposed. The initial flow is defined by eq. (6), in which α and S values are 0.056 and –0.47, respectively. The wavelength λ, which is supposed to keep unchanged in the whole shock course, is 10 mm, and the initial amplitude a_0 is determined by relative (on wavelength) ini-

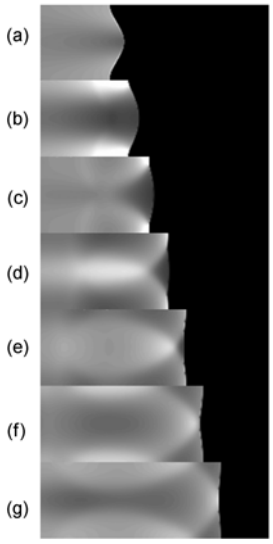

Figure 3 The pressure flow and its evolution.

tial amplitude a_0/λ (=0.02).

Figure 3 shows the typical pressure flow and its evolution. The initial pressure distribution is presented in Figure 3(a), and the pressure evolution with time is shown in Figures 3(b)–(g). It is clear that the pressure distribution behind the shock front is non-uniform, the amplitude of sinusoidal shock front damps over time, and the decay rate varies with the viscosity coefficient in viscous fluid. So the evolution of the shock wave is described by the oscillatory damping curve of the disturbance amplitude, defined by the relative amplitude (= a/a_0, the ratio of the disturbed amplitude a over the initial amplitude a_0) versus relative distance (= x/λ, the ratio of the propagation distance x of the shock front over the wavelength λ of the sinusoidal disturbance).

When the real viscosity coefficients value is zero, the disturbance amplitude damping curve by the present numerical method is shown in Figure 4, which is found to be independent of the artificial viscosity. Comparison with Miller and Ahrens' analytic solution indicates that good agreement is reached between them under the condition of small disturbance (a_0/λ=0.02). It demonstrates that the present numerical method gives the right solution for the development of shock waves with sinusoidal front.

The viscosity effects, when the shear viscosity coefficient η equivalent to the bulk viscosity coefficient κ, are also shown in Figure 4. During the early period, the disturbance amplitude quickly decreases, and the viscosity effects are not apparent. With the propagation of sinusoidally disturbed shock waves, the damping rate of amplitude slows down by viscosity effects in the later period. It is clear that both the phase of zero-amplitude point (the value of the relative distance at first position where the relative amplitude is zero) and the maximum amplitude of reverse-phase oscillation are sensitive to the real viscosity. When the viscosity coefficients rise, the zero-amplitude point is delayed; instead, the maximum amplitude of reverse-phase oscillation is reduced as shown in Figure 5.

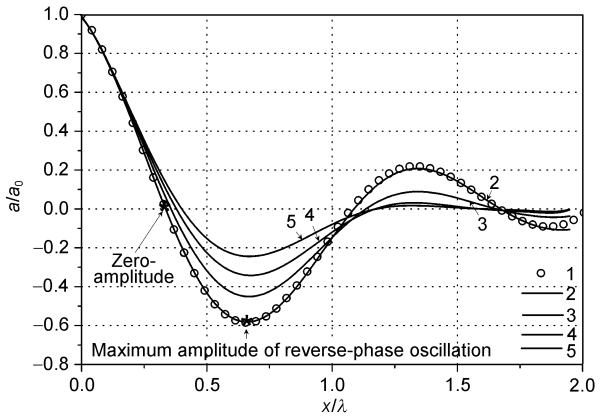

Figure 4 Disturbance amplitude damping curves of inviscid and viscous fluid. 1 is the inviscid analytic solution, 2 is the inviscid numerical solution, and 3, 4 and 5 are viscous numerical solutions respectively with viscosity (η=κ) 1000, 2000 and 3000 Pa s.

Below 200 Pa s the present numerical solutions for the phase change of the zero-amplitude point are basically consistent with those of Miller and Ahrens' analytic ones under the condition of small disturbance (a_0/λ=0.02), and their consistence is also reflected on the maximum amplitude of reverse-phase oscillation (in Figure 5(b)). But with further increase of viscosity, the discrepancy between them becomes larger and it shows that the analytic solution overestimates the phase increase of zero-amplitude point by 100% and reverse amplitude decreases by 30% at 2000 Pa s basically.

In our opinion, Miller and Ahrens' analytic solution does not give correct effects for higher viscosity, because (1) the hypothesis of shock waves with ideal discontinuity is not true for the actual flow of high viscosity [4,6–9,11–13], and (2) the abnormal enlargement of the disturbance amplitude at the initial stage and the occurrence of instability [5] in flow with higher viscosity are unreasonable [18]. The present numerical solution introduces the artificial viscosity as well as the inviscid model of the shock front, but the results are insensitive to it. It is pointed out that the numerical method can be applicable to the cases with more complicated initial flow and flows with higher viscosity, which is beyond the scope of the analytic solution of Miller and Ahrens. In Mineev's experiments [4,6–9], the initial ampli-

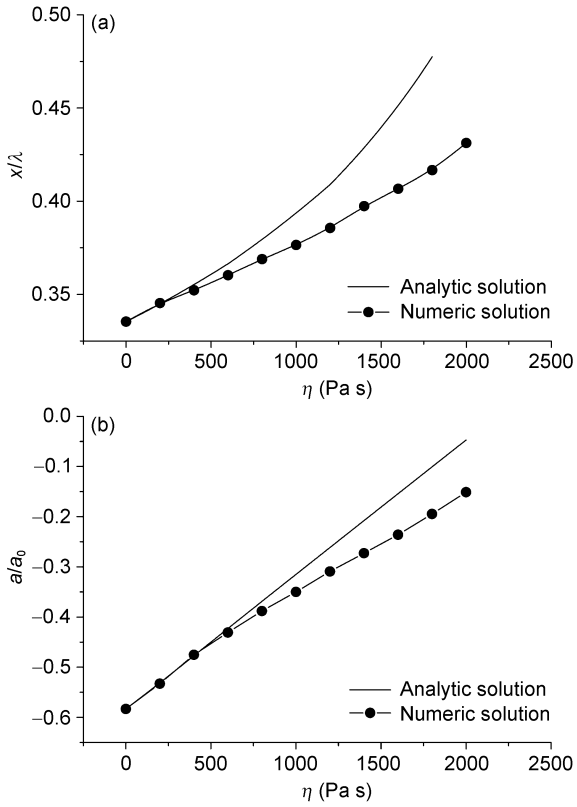

Figure 5 Effects of viscosity on the phase of zero-amplitude point (a) and on the maximum amplitude of reverse-phase oscillation (b).

tude is not small (e.g. a_0/λ=0.139), the analytic solution can not explain those data satisfactorily [5]. Whereas, the numerical solution is applicable to the situation of large disturbance and high viscosity, so it is expected to provide an effective analysis tool for the actual experiments [4,6–9, 11–13].

The above numerical solutions are for the oscillatory damping experiment about water shocked to 15 GPa by Mineev, etc. [7], unfortunately they did not give the disturbance amplitude damping curve data in their experiment. In the future, we will test our numerical solutions by experiments.

5 Conclusions

The finite difference method is firstly applied to obtain the numerical solution for amplitude damping curve of geometrical disturbance on shock front by solving two-dimensional hydrodynamic equations of Eulerian form for inviscid and viscous flow. A shock capturing scheme of maximum pressure gradient is adopted to locate the positions of the shock front, and the real viscosity in region behind the shock front is taken into consideration. For the non-uniform initial flow of Miller and Ahrens, the water shocked to 15 GPa is taken as an example. It is obvious that both the phase of zero-amplitude point and the maximum amplitude of reverse-phase oscillation are dependent on the real viscosity. The results are summarized as follows: (1) Under the condition of small disturbance (a_0/λ=0.02), the numerical method gives solutions in good agreement with the analytic one for inviscid and lower viscous fluid; (2) For the fluid of viscosity beyond 200 Pa s the analytic result is found to overestimate obviously the effects of viscosity. It is attributed to the unreal pre-conditions of analytic solution by Miller and Ahrens; (3) When the effects of higher viscosity in experiments of Sakharov and flyer impact are required to be evaluated the present numerical method can be used with more confidence, because the actual situations of larger disturbance amplitude, higher viscosity, and complicate initial flow can be in principle reproduced by numerical simulations. So the present numerical solution provides a path to overcome the bottleneck of viscosity measurement by the oscillatory damping method of shock waves.

This work was supported by the National Natural Science Foundation of China (Grant No. 10974160) and the National Science Foundation of China and Chinese Institute of Engineering Physics (Grant No. 10576025).

1 Buffett B A. Geodynamic estimates of the viscosity of the Earth's inner core. Nature, 1997, 388(6642): 571–573
2 Hide R. Motions of the Earth's Core and Mantle, and Variations of the Main geomagnetic Field. Science, 1967, 157(3784): 55–56
3 Secco R A. Viscosity of the outer core. In: Handbook of Physical Constants. Ahrens T J, ed. Washington: American Geophysics Union, 1995. 218–226
4 Mineev V N, Funtikov A I. Viscosity measurement on metals under shock-loading calculations for the earth's core. Physics-Uspekhi, 2004, 47(7): 671–686
5 Miller G H, Ahrens T J. shock-wave viscosity measurement. Rev Mod Phys, 1991, 63(4): 919–948
6 Sakharov A D, Zaidel R M, Mineev V N, et al. Experimental study of the shock wave stability and mechanical properties of materials at high pressures. Dokl Akad Nauk SSSR, 1964, 159: 1019–1022
7 Mineev V N, Zaidel R M. Viscosity of water and mercury under impact load. Zh Éksp Teor Fiz, 1968, 54(6): 110–118
8 Mineev V N, Mineev A V. Viscosity of metals under shock-loading conditions. J Phys IV France, 1997, 7(C3): 583–585
9 Mineev V N, Funtikov A I. measurements of the viscosity of water under compression. High Temp, 2005, 43(1): 136–145
10 Zaidel R M. Development of perturbations in plane shock waves. Prikl Matem Tekh Fiz, 1967, 4: 30–39
11 Liu F S, Yang M X, Li Q W, et al. Shear viscosity of aluminum under shock compression. Chin Phys Lett, 2005, 22(3): 747–749
12 Li Y L, Liu F S, Ma X J, et al. A flyer-impact technique for measuring viscosity of metal under shock compression. Rev Sci Insturm, 2009, 80(1): 013903
13 Li Y L, Liu F S, Zhang M J, et al. Measurement on effective shear viscosity coefficient of iron under shock compression at 100 GPa. Chin Phys Lett, 2009, 26(3): 038201
14 Mader C L. Explosives and Propellants. 2nd ed. Florida: CRC Press, 1998. 327–363
15 Von Neumann J, Richtmyer R D. A method for the numerical calculation of hydrodynamic shocks. J Appl Phys, 1950, 21: 232–237
16 Grady D E. Strain-rate dependence of the effective viscosity under steady wave shock compression. Appl Phys Lett, 1981, 38: 825–826
17 Mitchell A C, Nellis W J. Equation of state and electrical conductivity of water and ammonia shocked to the 100 GPa (1 Mbar) pressure range. J Chem Phys, 1982, 76: 6273–6281
18 Morduchow M, Paullay A J. Stability of normal shock waves with viscosity. Phys Fluids, 1971, 14(2): 323–325